ELSEVIER

Chemical Engineering Science 63 (2008) 2641–2656

Chemical Engineering Science

www.elsevier.com/locate/ces

Experimental validation of a rigorous desorber model for CO_2 post-combustion capture

Finn Andrew Tobiesen[b,*], Olav Juliussen[b], Hallvard F. Svendsen[a]

[a]*Department of Chemical Engineering, Norwegian University of Science and Technology, NTNU, N-7491 Trondheim, Norway*
[b]*SINTEF Materials and Chemistry, N-7465 Trondheim, Norway*

Received 8 October 2007; received in revised form 4 February 2008; accepted 6 February 2008
Available online 14 February 2008

Abstract

A numerical model for CO_2 desorption including desorber packing, reboiler, and condenser was developed and validated against pilot plant data. Mass transfer data for both liquid and gas were obtained. Runs with pure water enabled check of the heat balance and estimation of the heat losses in the unit. The agreement between the experimental averaged and the simulated CO_2 mass transfer rate was found to be good, with an average absolute deviation (AAD) and absolute deviation (AD) of 9.92% and 9.91%, respectively. The simulations slightly over-predict mass transfer in the low loading ranges and under-predict mass transfer in the high loading range. In addition, simulated and measured desorber temperature profiles agree very well for the low loading ranges where the desorber inlet liquid flow was well characterized. In cases where flashing of the desorber inlet flow occurs, it was found extremely important to know the enthalpy content. Desorber rich end pinches were found for most of the runs at low and medium loading. Using four different equilibrium models, it was shown that a simplified and a rigorous model would give very similar desorption performance predictions. The activity coefficient of water was found to have a strong influence on the agreement with experimental data.

Keywords: CO_2 absorption; Desorber model; Experimental validation; Laboratory pilot plant; MEA

1. Introduction

Carbon dioxide (CO_2) separation by absorption with chemical reaction is often considered to be the most cost effective and viable option for large-scale CO_2 removal from flue gases. A schematic diagram of a typical amine regeneration process, represented by the pilot plant used, is shown in Fig. 1. However, the energy requirement in these processes is today too high to make the technology feasible on a global scale. In a conventional plant, over 80% of the total energy required, using monoethanolamine (MEA) as an absorbent, is consumed in the regeneration step (Chakma, 1999). In order to achieve energy requirement reductions, the desorber should be the primary target and as a tool, a thoroughly validated simulation model is necessary.

In this study, the amine regeneration section of a simulation program, capable of modeling the whole absorption/desorption process, is validated against detailed pilot plant data. This work follows the validation study undertaken on the absorber section and the experimental set-up is as described in a previous paper (Tobiesen et al., 2007).

In terms of models found in the literature, the paper by Weiland et al. (1982) deals with thermal desorption of CO_2 from MEA in a packed column, the paper by Bosch et al. (1990) describes desorption of acid gases (CO_2 and H_2S) from loaded alkanolamine solutions, the paper by Glasscock and Rochelle (1991) describes CO_2 absorption and stripping from a mixture of amines, and the paper by Kershenbaum et al. (1991) study the thermal desorption of CO_2 from MEA solutions in a plate column. Astarita and Savage (1980a, b) describe in detail the interfacial mass transfer modeling for desorption with chemical reaction. Cadours et al. (1997) made kinetic measurements on desorption of CO_2 in aqueous MDEA solutions.

Although various models have been proposed for acid gas absorption with the use of amines, only a few include the desorber and reboiler. Even fewer are supported with pilot

* Corresponding author. Tel.: +47 98283947; fax: +47 73592786.
E-mail address: Andrew.Tobiesen@sintef.no (F.A. Tobiesen).

0009-2509/$ - see front matter © 2008 Elsevier Ltd. All rights reserved.
doi:10.1016/j.ces.2008.02.011

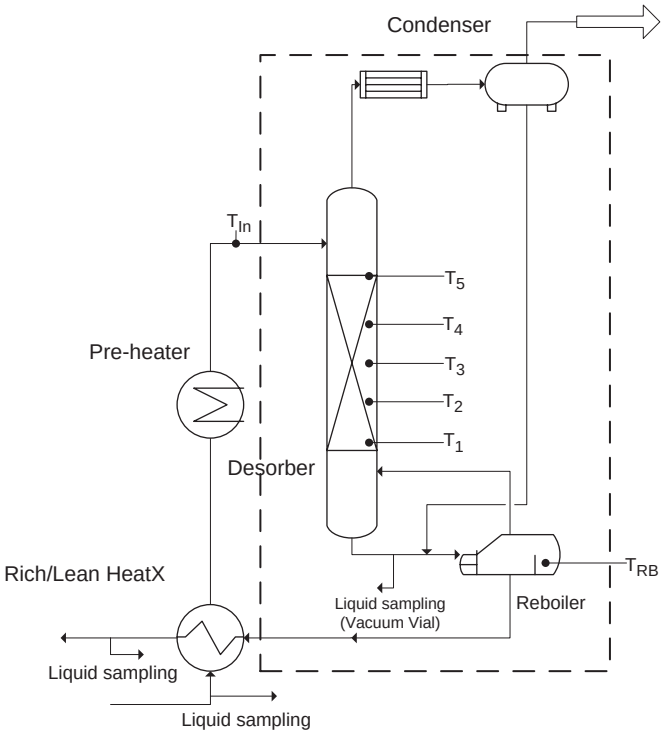

Fig. 1. Simplified flow sheet of amine regeneration units.

plant data. The regeneration part of the absorption process is considerably more complex than the absorber, both regarding the modeling as well as the evaluation of the obtained results. In addition to the desorber packing section separate models of the reboiler and condenser are needed in the modeling flowsheet. It is of importance to have detailed models of such processes to understand the underlying mechanisms associated and to add to our understanding of this process.

2. Model theory

2.1. The flow model

The description of the flow model for the desorber packing is identical to the absorber packing model presented in a previous paper (Tobiesen et al., 2007) and is not described here. The model was originally written with the intention of being able to solve numerically stiff problems that often arise when attempting to simulate a desorber packing. This occurs because of the very fast reaction rates at the interface as well as large heat transfer numbers due to the elevated temperature in the desorber.

2.2. Gas/liquid mass transfer model

In desorption with chemical reaction, the reversibility of the reaction is the main driver for the mass transfer. The theory for absorption with chemical reaction that takes reversibility into account can be used for desorption, as long as no a priori assumption about the direction of the driving force is made (Astarita and Savage, 1980a).

The desorber can be modeled by the use of finite rates for chemical diffusion and reaction. In such a case, the system of differential equations, as described by the penetration theory (Tobiesen et al., 2007), describes the process and thus no empirical correlation for the liquid side physical mass transfer coefficient is needed. In such a case, only a correlation for the liquid contact time is needed. However, this procedure requires a finite rate equation for the reactions occurring under desorption conditions. At these conditions very little data exist to allow reaction rate evaluations. Furthermore, the computational cost of solving the set of partial differential equations is high. Because of this, mass transfer with a reversible instantaneous reaction is assumed taking place in the desorber. If this is the case, chemical equilibrium prevails everywhere in the liquid phase (Astarita and Savage, 1980b). MEA is used as an example in the following and also the experimental study was performed with MEA as the absorbent.

For the reaction

$$A + \sum v_j B_j = 0, \tag{1}$$

Astarita et al. (1980b) showed that the enhancement factor can be found as the solution to

$$\xi = (E-1)(C_A^{\text{in}} - C_A^b), \tag{2}$$

where the parameter ξ is the solution to

$$\frac{C_A^{\text{in}}}{C_A^b} = \prod_j \left(1 - \frac{v_j \xi}{r_j B_j^b}\right)^{v_j}, \tag{3}$$

where C_A^{in} is the interface concentration and C_A^b the bulk concentration of the absorbing component (solute), e.g. CO_2. The ratio $r_j = D_j/D_A$ is the ratio of absorbent to solute diffusivity and j is the number of species other than the absorbing component.

Chemical equilibrium is assumed to be at the interface through the dependency of Henry's law. The enhancement factor therefore depends on the bulk-concentrations of C_A^b, B_j^b, and the interface concentration C_A^{in}, and is independent of the equilibrium constant for the chemical reaction. However, one of the liquid-phase concentrations can be replaced by the use of the equilibrium constant for the overall reaction. The enhancement factor for the instantaneous reversible reaction at equilibrium for CO_2 and MEA is given by (Danckwerts, 1971)

$$E = 1 + \frac{\dfrac{D_{\text{MEACOO}^-}}{D_{\text{CO}_2}} \sqrt{K} C_{\text{MEA}}^b}{\left(1 + 2\dfrac{D_{\text{MEACOO}^-}}{D_{\text{MEA}}} \sqrt{K C_{\text{CO}_2}^{\text{in}}}\right)\left(\sqrt{C_{\text{CO}_2}^{\text{in}}} + \sqrt{C_{\text{CO}_2}^b}\right)}, \tag{4}$$

where C_{MEA}^b is the bulk concentration of free MEA and $C_{\text{CO}_2}^b$ is the free CO_2 bulk concentration, which are both obtained from the equilibrium model. $C_{\text{CO}_2}^{\text{in}}$ is the interfacial liquid side concentration of CO_2 at equilibrium with the gas phase. The enhancement factor model assumes equal diffusion coefficients for protonated amine and carbamate.

This expression is identical to the expressions obtained by Olander (1960) and Danckwerts (1971).

The expression for the interfacial CO_2 flux is here expressed by using activities for the driving force (Tobiesen et al., 2007)

$$N_{L,k} = Ek^0_{L,k}(\gamma^{\text{in}}_k C^{\text{in}}_k - \gamma^{b,\text{eq.}}_k C^{b,\text{eq.}}_k) \quad (5)$$

and

$$N_{G,k} = k_{G,k}(P^b_k - P^{\text{in}}_k), \quad (6)$$

where

$$P^{\text{in}}_k = H_k \gamma^{\text{in}}_k C^{\text{in}}_k. \quad (7)$$

The physical mass transfer coefficients $k^0_{L,k}$ and $k_{G,k}$ can be obtained from the literature for the specific packing. These are correlated at low-to-medium temperature and not verified for desorber conditions. It can be noted that activity coefficients have been incorporated into the driving force expression as they represent a significant contribution, whereas the enhancement factor model has not been reevaluated. The enhancement factor model also does not include the formation of bicarbonate, even though the thermodynamic models do. This will have only a very limited effect at desorber conditions.

The interfacial mass transfer flux can be found by iteration with residue: $N_{L,k} - N_{G,k}$. This approaches zero when the concentration at the interface $C^{\text{in}}_{\text{CO}_2}$ approaches the correct value according to the mass balance relationships. This routine is faster than solving the penetration model since there is only one iteration variable, the total concentration of CO_2 at the interface. The thermodynamic model must be called for every new guess for the interfacial and liquid bulk CO_2 activity and concentration and for each step in the packing section.

The interfacial sensible heat transfer is modeled using a simple heat transfer coefficient approach where the heat transfer coefficient is deduced from the mass transfer coefficient and the Chilton–Colburn analogy (Bird et al., 1960).

3. Numerical scheme

3.1. Optimizations for solving the desorber packing

In order to reduce the heavy computational effort for solving the packing, since the mass transfer model must be solved at every call from the flow model, two methods can be used. The first involves evaluation of the Jacobian, where the previous determined interfacial flux can be used when obtaining the function derivatives. This reduces the number of calls to the mass transfer model significantly. The second method is based on the difference of the values of the variables between two calls. If the functional variables in the mass transfer modules change less than a given limit from the previous call, the previous flux can be used. The limit is chosen such that the overall stability is not jeopardized.

3.2. Use of continuation in solving the packing model for the desorber

Since the desorbing reaction rates are very high, the gradients in certain areas of the desorber become large and the problem can become difficult to solve numerically. Furthermore, the quality of the initial guess for the vapor stream from the reboiler is critical for the performance of the numerical approach or if a solution can be obtained at all. In order to solve this problem, the present model starts with an initial guess of the vapor flow into the desorber packing which is made easy to solve by reducing the heat and mass transfer coefficients. A new initial guess is obtained, from an overall mass balance, and the heat and mass transfer coefficients are adjusted one step towards their actual values. This is continued and after a specified number of iterations the heat and mass transfer coefficients have reached their correct values. Normally, after 7–8 iterations the total mass and heat balances around the desorber/condenser and reboiler are converged. In such a manner, the regions in the desorber that exhibit very fast numerical variations can be solved fairly easily, but at the cost of a larger number of iterations around the desorber. A block diagram showing the solution sequence is shown in Fig. 2.

3.3. Controlling reboiler vapor production

A recycle loop is used to close the energy and material balances around the reboiler and condenser. This requires proper consideration of initial guesses, in particular a careful choice of bounds for the boil-up stream guess, which are iterated towards solution through the overall balance criteria. An initial "good" guess for the recycle loop is obtained by using a reasonable guess for boil-up based on the amount of liquid flowing into the reboiler. This is important in order to obtain a solution when using very low reflux rates, i.e. low reboiler duties. A consequence of a low reboiler duty at a given pressure and circulation rate is that only a very limited amount of steam is generated. In other words, it is important to be above the bubble point to ensure that some amount of steam is produced at each successive iteration around the desorber packing.

3.4. Thermodynamic model

The equilibrium between the species in the vapor and liquid phases was obtained, for the base simulation model, from the model described previously (Tobiesen et al., 2007; Hoff et al., 2004) where the model is fitted to own experimental VLE data from 40 to 100 °C as well as the data at 120 °C given by Ma'mun et al. (2005). The model was also fitted to the data of Jou et al. (1995). In addition, the Deshmukh–Mather model (Deshmukh and Mather, 1981) was implemented with the interaction parameters given by Weiland et al. (1993) as well as with parameters tuned to own data at 40–100 °C and data at 120 °C of Ma'mun et al. (2005).

3.5. Correlations for hydraulic properties of packing

The mass transfer correlations used were taken from Rocha et al. (1993, 1996) and the effective interfacial area was obtained from De Brito et al. (1994). The correlations for liquid holdup and limits for flooding were obtained from Billett and

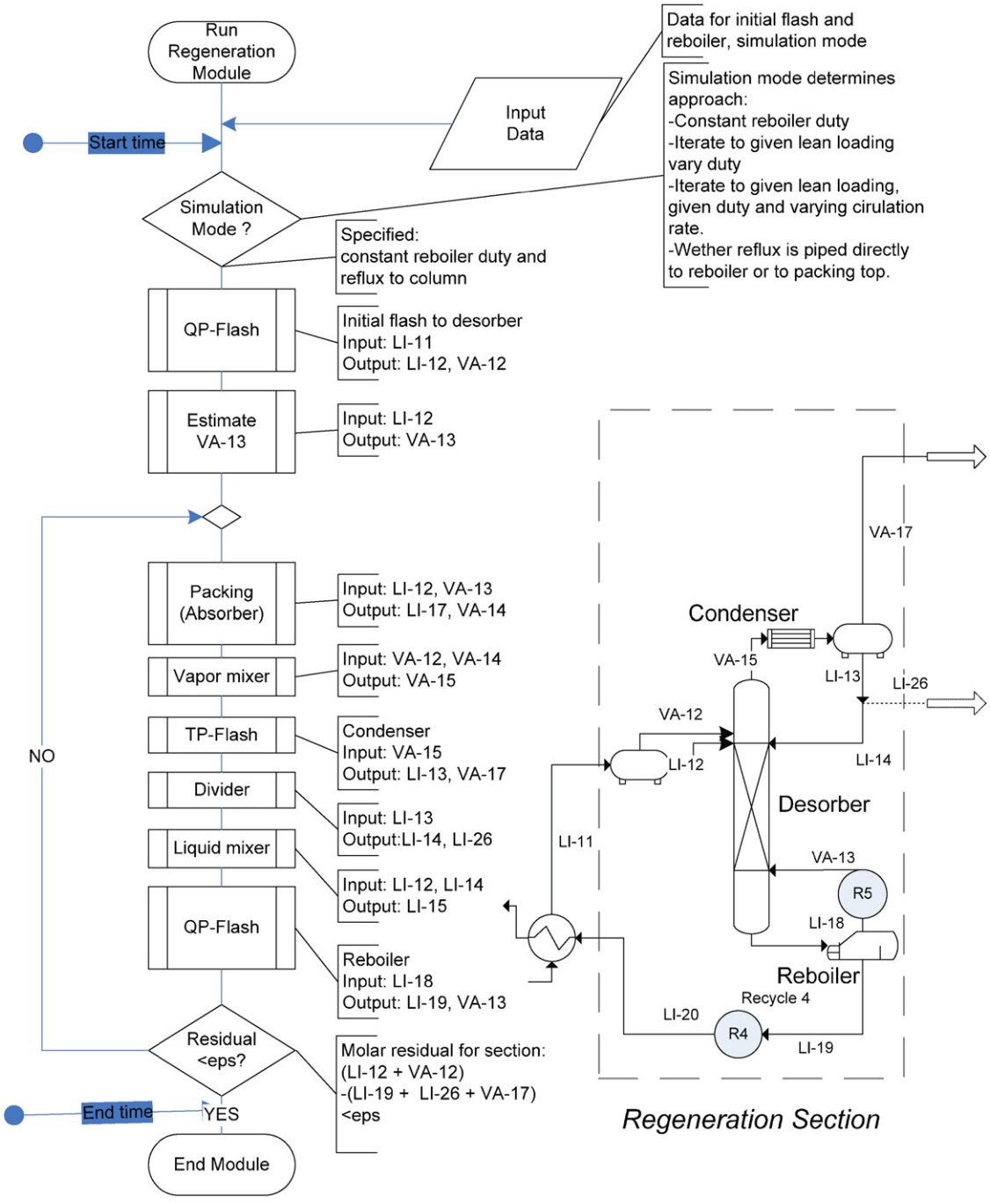

Fig. 2. Block diagram of the solution algorithm for the amine regeneration unit.

Schultes (1999), respectively. These are described in more detail in Tobiesen et al. (2007) and in Section 5.

4. Experimental installation

4.1. Desorber operation and measurements

The data were obtained in conjunction with the absorption data described in Tobiesen et al. (2007). A schematic of the integrated pilot plant is shown in Fig. 1 and the operating conditions and contactor data for the desorber are given in Table 1. The runs contain a liquid load varying from 5 to 17 $m^3/(m^2h)$, rich loadings varying from 0.30 to 0.45, and lean loadings in the range 0.18–0.4. The experimental data were gathered over a time span of three months of continuous operation. The plant desorber has 0.10 m ID and 4.1 m packing height and is fitted with a reboiler with 18 kW maximum capacity. The packing is Mellapak 250Y and the system is capable of removing about 10 kg CO_2 per hour. The verification analysis in this work is focused only on the amine regeneration section of the pilot plant. The condenser reflux is piped directly to the reboiler. The entire regeneration section was insulated to minimize heat loss

Table 1
Contactor- and operating data

Desorber	
Column internal diameter (m)	0.1
Main packing height (m)	3.89
Packing (structured)	Sulzer Mellapak 250Y
Parameter	**Value**
Gas flow rate (m^3/h)	150
Liquid circulation rate (L/min)	3–9
MEA concentration (wt%)	30
Rich loading (mol CO_2/mol MEA)	0.30–0.45
Lean loading (mol CO_2/mol MEA)	0.18–0.40
Inlet liquid temperature stripper (°C)	105–115
Reboiler temperature (°C)	110–125
Reboiler heat duty (kW)	3–13.5
Desorber pressure (kPa a)	~ 200
Condenser temperature (°C)	~ 15

to the surroundings. To estimate the heat loss in the units, the pilot rig was operated with water and reflux rates were measured at fixed reboiler duties. In addition, insulation surface temperatures were measured and the heat loss was estimated from this. In this manner, the reflux rates could be compared with the electric duties of the reboiler. In total, 19 experimental runs were recorded. In addition, six runs were performed with pure water in the pilot rig in order to measure the amount of reflux produced at a given reboiler duty and to estimate the pilot plant heat loss. The reflux rate was measured using a mass flow meter.

4.2. Measurements

Determination of solvent and gas composition as well as calibrations and data acquisition strategy is described in Tobiesen et al. (2007). The desorber liquid samples were taken from the unit via pressure vials to minimize chances of CO_2 flashing at the elevated temperature. Each time liquid samples were withdrawn from the system for analysis, operational data were obtained by averaging over a 30 min interval around the sampling time. After a change in operational conditions, the plant was run for at least 5 h to ensure steady-state operation. After attaining steady-state conditions, indicated by steady temperature profiles and constant pressures around the regenerator sections, liquid samples were taken from the rich desorber inlet, the lean amine desorber outlet, and the lean amine reboiler outlet. The sampling points are shown in Fig. 1. The CO_2 gas flow rate after the condenser was measured using a mass flow meter. The temperature probes in the packing were calibrated to a precision of about 0.1 °C with a Beamex calibrator. Inlet liquid temperature to the desorber was calibrated to whole degrees.

5. Results and discussion

5.1. Desorber operation with pure water

Reboiler, stripper column, and all connected pipes were thoroughly insulated in the pilot plant. It is, however, of interest to find the regeneration system heat loss by analyzing the water balance as well as comparing measured temperatures and pressures for the one component system and to simulated values. In Fig. 1 the boundary for the heat balance is given by the dotted line and in Fig. 3 the experimentally obtained reflux rates for the six water runs compared with the simulated ones are shown. In these simulations with water, the same unit operations are included as for the later CO_2/amine modeling cases. The experimental input data used in the simulations were the inlet water flow (rate, temperature), condenser liquid outlet temperature, as well as the reboiler pressure and heat duty. The values to compare are thus condensate flow rate and reboiler temperature. In Fig. 3 two series are shown. One shows simulated reflux rates assuming that the regeneration units operate adiabatically, while the other shows simulation results when an estimated heat loss from stripper and reboiler is included. The heat losses were estimated by measuring the surface temperature of the insulated and Al-foil clad stripper and reboiler. Heat losses due to natural convective and radiative heat transfer were then computed. The heat flux from the stripper was estimated to be 110 W/m^2 and the heat loss from the reboiler was 220 W/m^2. The heat loss from the stripper was included in the external heat loss term in the packing model while the loss in the reboiler was subtracted from the reboiler heat duty. The total heat loss from the stripper and reboiler was estimated to be less than 0.5 kW. Fig. 3 shows that the computed reflux rates obtained agree well with the measured values for all runs. It can be noted that the adiabatic results show the smallest experimental deviations, whereas the runs including the estimated heat loss show a small average under-prediction of reflux rates. This is contrary to what would be expected. The interval between each experimental steady state was around 30 min. The temperatures were then steady but some variations in the measured reflux rates were observed and averages over a time span of 5–30 min were calculated. Taking into account the uncertainties in input data (reboiler duty and inlet water flow rate and temperature) the two simulation cases were deemed equally

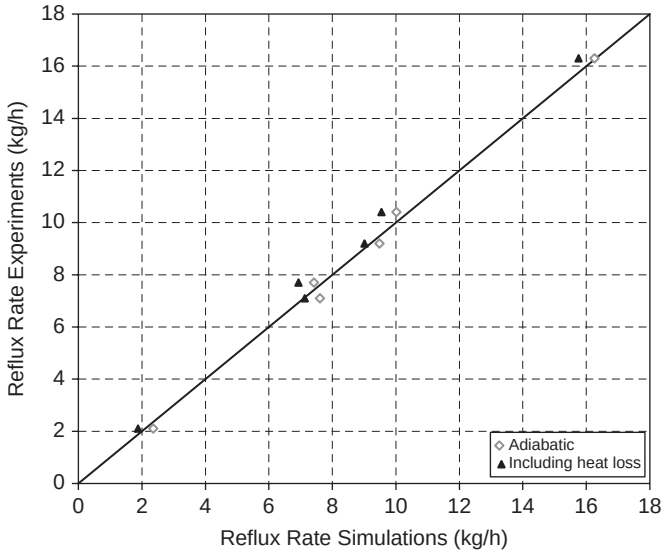

Fig. 3. Experimental and simulated reflux rates from pilot rig run with water.

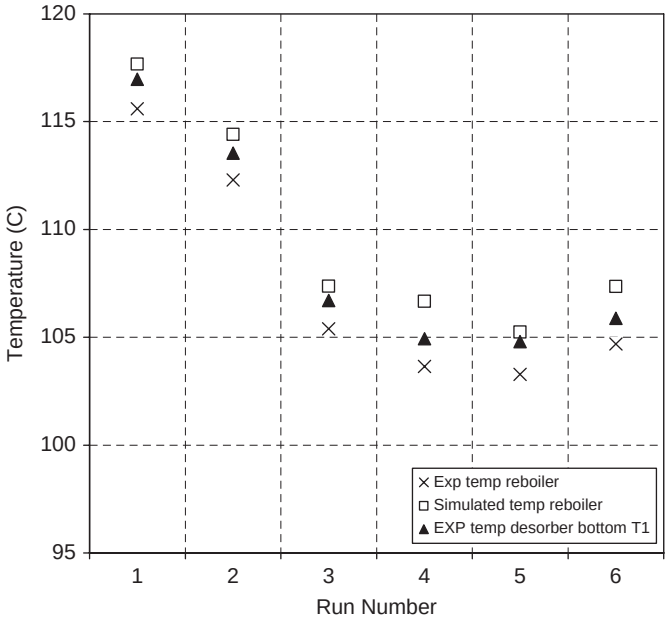

Fig. 4. Experimental and simulated reboiler temperatures from pilot rig run with water.

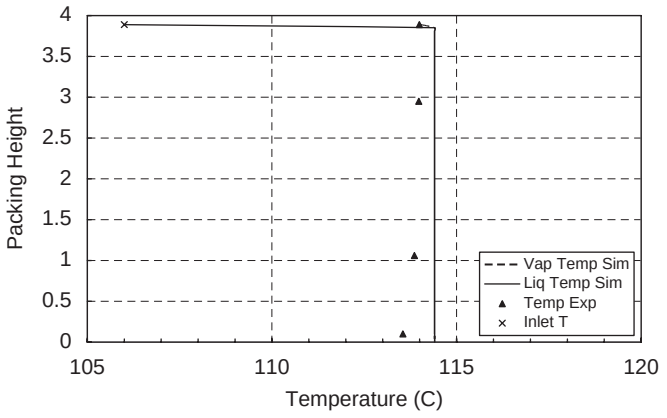

Fig. 5. Experimental and simulated packing temperatures from pilot rig run 2 with water.

good. A heat loss is inevitable since the skin temperature of the insulation was about 50 °C for the reboiler and about 35 °C for the stripper. It was therefore concluded that the independently estimated heat losses from the desorber and reboiler were trustworthy and were accounted for by inclusion in the simulation model.

Fig. 4 shows a comparison of the calculated reboiler temperature at the given duty and measured pressure with the measured reboiler temperature for the same runs. Three values are shown: one is the simulated reboiler temperature, the other is the measured reboiler liquid temperature (T_{RB}), and the third is the temperature from the probe at the desorber bottom (T_1). The figure shows that the simulated reboiler temperatures deviate systematically from the measured reboiler temperatures. The simulated values are generally 2–2.5 °C higher than the measured values. The reboiler was specified by duty and pressure, both measured values. In a one-component system with pressure given, the boiling point temperature is determined. The discrepancy between the simulated and experimental values can be caused either by an error in the pressure measurement in the reboiler, by inert gas in the system, or by errors in the temperature measurement. It should be noted that the temperatures in the reboiler are generally 1–2 °C lower than the measured temperatures at the first point in the desorber packing, 10 cm above the packing entrance. The opposite would be expected. The pressure measurements were calibrated and have an accuracy of $< \pm 2$ kPa. This gives a boiling point uncertainty of $< \pm 0.3$ °C, which is negligible. In addition, the presence of inert gas in sufficient quantities to explain the difference ($\sim$ 5–10%) is highly unlikely and would also affect the desorber bottom temperature. It is also expected that the inaccuracies in the correlations for the ideal enthalpy and saturation pressure of water used in the simulation model are very small. This points to an error in the reboiler temperature reading of about 2–2.5 °C, which could be caused by the temperature probe position.

Fig. 5 gives the desorber temperature profile. Because of the low pressure drop in the desorber, it is almost flat. The measured temperatures in the packing are systematically about 0.5 °C lower than the simulated temperature. A small inert gas content of about 1.5% could explain this discrepancy and such a content is possible. From the figure it can be shown that the inlet liquid temperature (inlet T) to the packing is 106 °C, whereas at the top of the packing the temperature (T_5) is 114 °C. The inlet is placed about 30 cm above the packing and the liquid heats up rapidly to the temperature at the packing top. In Fig. 5 the inlet liquid level is placed at the top of the packing, but should in reality be at position 4.2 m. This has no effect on the simulation.

From these analyses it can be concluded that the model predicts the water system well and within the experimental uncertainties.

5.2. *Evaluation of experimental data with* CO_2 *desorption*

Tables A1 and A2 list all input and measured data for the 19 runs recorded for the regeneration units. Unfortunately, it was not possible to measure the steam flow from the reboiler to the desorber using a flow meter because of a large pressure drop in the instrument. Therefore, the steam boil-up could not be compared with the simulated results. However, the desorber outlet liquid was analyzed and thereby the desorber and reboiler could be analyzed independently.

Fig. 6 compares experimental data for the individually obtained total liquid side CO_2 removal in the desorber and reboiler together with the gas side CO_2 production. The liquid side CO_2 removal is calculated as the difference between the CO_2 rate in the incoming liquid to the desorber and in the liquid exit from the reboiler. The gas side CO_2 production is measured with a mass flow meter downstream the condenser. Fig. 6 shows that the mass balance agreement between the gas and the liquid sides is very good. For most points it is within 3% and only two points show more than 10% deviation.

Table 2 gives the average absolute deviation (AAD) and absolute deviation (AD) for the data set. Using all data points from the 19 runs gives an AAD of 4.21% and an AD of 4.48%. The very low deviation values for such a complex system are deemed acceptable and can be taken as a support for the quality of the experimental data. The figure also shows that for the runs in loading ranges 1 and 2, i.e. loading < 0.4 in inlet rich loading, the mass balance agreement is excellent. For range 3, i.e. loading $\geqslant 0.4$, the gas side measured values are slightly higher than the liquid side measured value. The reason for this is uncertain, but one possible cause could be loss of CO_2 in the sampling of the rich amine, and thus a too low inlet CO_2 concentration. Even though the rich and lean liquid sampling is done on the cold side of the heat exchanger, some flashing of the rich amine could occur. At this point it is difficult to tell which data set is better (liquid or gas), and in the subsequent simulation comparisons, an average of the values is used.

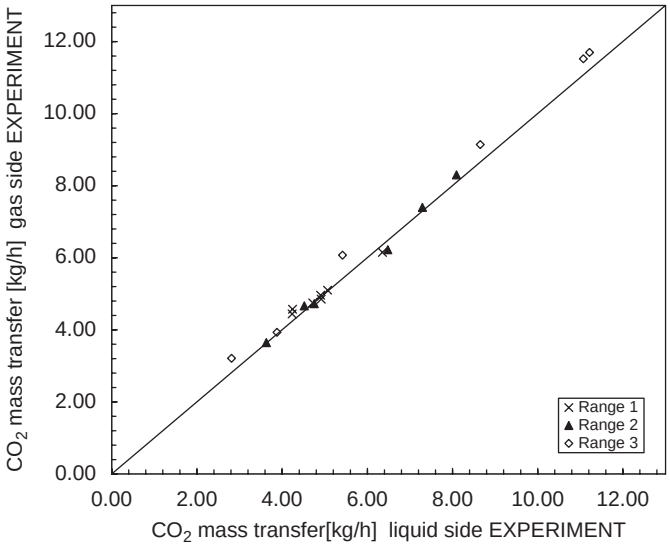

Fig. 6. Experimental CO_2 production rates (kg/h), calculated based on the gas and liquid analysis: ×, loading range 1: $y_{rich} < 0.32$; ▲, loading range 2: $0.32 \leqslant y_{rich} < 0.4$; ◇ loading range 3: $y_{rich} \geqslant 0.4$.

Table 2 also gives data for the reboiler heat duty, given as $MJ/kg\,CO_2$ removed. It can be seen that the absolute values of the steam consumption range from 11.2 to $3.7\,MJ/kg\,CO_2$ removed. The highest values are found for the cases with low inlet liquid CO_2 loading (0.26–0.29) and reflect the higher energy demand when approaching low loadings in the lean amine. This is consistent with the results from other simulations and experimental results pointing to an optimum lean loading in the range of 0.23–0.27 mol CO_2/mol MEA (Burkhardt et al., 2006; Sakwattanapong et al., 2005). At higher loading the reboiler heat duty goes down to $\sim 3.7\,MJ/kg\,CO_2$ removed, reflecting the relative ease with which CO_2 desorbs in this range.

The performance of the stripper and reboiler can also be evaluated individually by using the desorber outlet composition measurement. The data for desorber inlet, outlet and reboiler

Table 2
Mass transfer of CO_2, mass transfer deviation, AD and AAD for the experimental runs

Run[a]	Loading range	Rich loading (mol/mol)	Lean loading (mol/mol)	Absorbed CO_2 liquid (kg/h)	Absorbed CO_2 gas (kg/h)	% dev Abs CO_2 x_i[b]	Steam consumption (MJ/kg)	%-stripping desorber[c]
1	1	0.32	0.22	5.07	5.10	0.63	8.22	49.8
2	1	0.32	0.22	4.90	4.96	1.12	8.47	71.3
3	1	0.31	0.22	4.92	4.85	1.38	8.48	60.4
4	1	0.31	0.22	4.72	4.75	0.61	8.82	48.1
5	1	0.26	0.18	4.24	4.44	4.79	11.21	62.8
6	2	0.37	0.28	6.48	6.22	3.95	6.58	46.0
7	1	0.29	0.24	3.82	4.57	19.69	9.64	32.1
8	1	0.31	0.23	6.35	6.15	3.20	7.95	55.1
9	2	0.33	0.21	4.52	4.67	3.16	7.52	67.6
10	2	0.34	0.22	4.75	4.72	0.59	7.37	63.7
11	2	0.40	0.30	3.63	3.64	0.48	5.74	40.8
12	2	0.39	0.29	8.09	8.30	2.57	5.09	51.1
13	3	0.45	0.38	2.81	3.21	14.14	4.66	45.6
14	3	0.46	0.37	11.07	11.52	4.02	3.70	60.9
15	3	0.45	0.40	3.88	3.93	1.35	5.34	23.7
16	3	0.45	0.41	5.42	6.07	12.06	4.95	17.1
17	3	0.43	0.34	11.21	11.70	4.30	4.21	40.5
18	3	0.41	0.34	8.65	9.14	5.68	4.74	52.5
19	2	0.35	0.29	7.29	7.39	1.37	6.67	46.3
AAD						4.21		
AD						4.48		

[a] Sorted by date.
[b] $x_i = \frac{v_{sim} - v_{ex}}{v_{ex}} \cdot 100$.
[c] Percent stripping in desorber compared with reboiler.

outlet loading are summarized in Table A1. From this the percentage of CO_2-stripping taking place in the desorber can be calculated. Runs 1–4 are performed with almost identical liquid load, heat duty, and inlet CO_2 loading, see Table A2. They show that the total amounts of CO_2 stripped, based on the reboiler outlet loading, are almost identical. However, the desorber outlet loadings vary significantly, resulting in amounts stripped in the desorber varying between 48% and 71% as shown in Table 2. The sampling of the liquid outlet of the desorber was done using a pressure vial to prevent flashing at the elevated temperature and pressure. The experimental uncertainty associated with the loading of this stream is therefore slightly higher than for the desorber inlet and reboiler outlet samples, which were both sampled at low temperature and pressure. Probably this is the cause of the variations seen, implying that the results do not indicate real variations in the operating values. An error in these readings would probably only go in one direction as flashing during sampling can occur whereby CO_2 is lost. This results in too low desorber outlet loadings being measured, meaning a too high percentage stripped in the desorber. However, we have much experience in such sampling and all possible was done to avoid it. The uncertainty is probably not more than ±4–5%. However, it should be noted that because of the low degree of stripping, small uncertainties in the loading measurements, and in particular for the desorber outlet loading, will lead to large uncertainties in the percentage stripped in the desorber section. For example, ±4–5% translates to ±0.01–0.02 in loading. It is thus extremely hard, if at all possible, to obtain sufficient accuracy in the desorber outlet loading reading to justify a detailed comparison with simulated values.

Some reasonably well-founded conclusions can, however, be drawn. The degree of stripping in the desorber column compared with reboiler seems to decrease with increasing rich loading. When this effect can be seen comparing runs 6, 7, and 12, runs 9 and 10, and runs 17 and 19. However, for runs 14 and 18 the opposite is true. A trend line through the whole data set shows the former effect.

It also seems that the percentage CO_2 removed in the desorber decreases with decreasing heat duty. This can be seen when comparing run 16 with 17, run 15 with 6, 7, and 12, and run 11 with 9 and 10. This may not be surprising since at low boil-up rates the somewhat colder desorber inlet liquid will affect the desorber more than at high boil-up rates.

5.3. Basis for validation of amine regeneration unit model

All the obtained experimental data from the pilot plant regeneration section were used with the corresponding simulation results as the basis for model validation. The following experimental data were used as input basis for the model verification for the regeneration unit:

- The incoming liquid stream to the desorber packing, molar flow rate, component molar composition, temperature, and pressure.
- The reboiler heat duty and pressure.
- Lean loading out of reboiler.
- Condenser temperature and pressure.
- Packing dimension and type.
- Reboiler efficiency. As base case 100% was used.
- The heat losses in the desorber and reboiler, respectively, as mentioned earlier, were included.

Since there was no way of measuring whether, or the degree to which, the rich amine stream into the desorber was single- or two-phase, an assumption regarding this had to be made. It was also not known whether this inlet liquid stream was at equilibrium. The stream either could be assumed being pure liquid phase at the measured inlet temperature, and thus not necessarily in equilibrium, or it could be assumed in two-phase at equilibrium determined by an equilibrium calculation at the measured inlet temperature. A combination between these two extremes would also be possible. Taking into account the vertical distance from the desorber inlet to the rich/lean heat exchanger, being about 4 m, it is very unlikely that the stream is a single-phase liquid if equilibrium should predict otherwise. However, a two-phase equilibrium situation at the inlet would be predicted only for the high rich loading range. Therefore, in order to have a consistent basis and in spite that we know that this may not be correct for some of the high loading runs, the basis for the experimental determination of the inlet rich enthalpy content was taken as single-phase liquid at the measured inlet desorber temperature. The effect of making the other choice (inlet at equilibrium) is also shown and discussed. The cross-flow heat exchanger as part of the amine regeneration section was considered to be included in the modeling work. This could give more data for comparison, as both the rich stream into the heat exchanger and the lean stream out of the heat exchanger would be single phase and with known composition and temperature. However, the temperature of the outlet lean stream was not measured in the present campaign and therefore the degree of uncertainty around the enthalpy content of the inlet stream would remain just as high.

Using these data as input, the amine regeneration section could be simulated and compared with the analyzed liquid and gas streams from the pilot rig. The temperature profiles could also be compared with the five temperature measurements in the desorber packing.

As interfacial mass transfer model, an enhancement factor model with instantaneous reversible reaction was implemented as described earlier, using CO_2 activities in the expression for the CO_2 driving force. The correlations for thermal data, such as gas- and liquid-phase enthalpies, and CO_2 heat of absorption were the same as those used in Tobiesen et al. (2007). As base case, the explicit equilibrium model of Hoff et al. (2004) as given in Tobiesen et al. (2007) was used.

5.4. Comparison between experiments and base case model predictions

5.4.1. CO_2 desorption

In Fig. 7 a comparison between the experimental averaged and the simulated CO_2 mass transfer rates is given for the

base case using simulation mode 1. The general agreement can be seen to be good. The spread around the diagonal is a good indication that there is no systematic discrepancy between model and experiments for the data set as a whole. This is clearly shown in Table 3 for the base case where AAD and AD are found to be 9.92% and 9.91%, respectively. The level of less than 10% average deviation is deemed good in these tests. However, when considering the loading ranges separately, it is seen that the simulations tend to slightly over-predict mass transfer in the low loading ranges 1 and 2 and under-predict mass transfer in the high loading range. The under-prediction for the high loading ranges is discussed later.

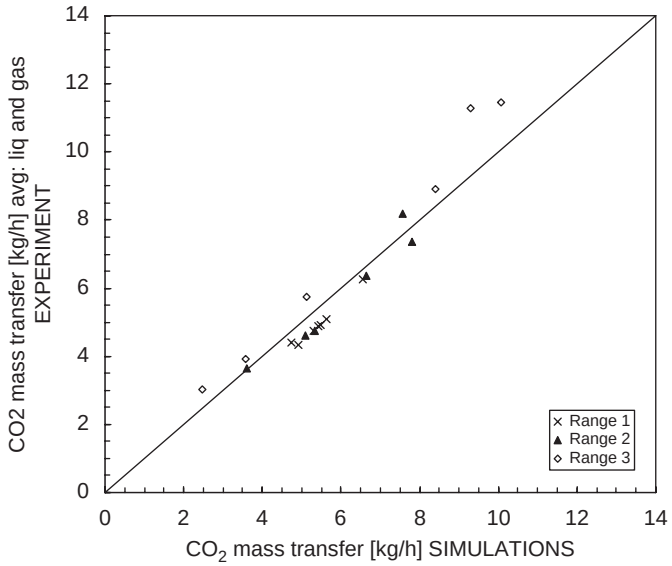

Fig. 7. Experimental CO_2 mass transfer in desorber and reboiler based on the average gas and liquid side versus simulations.

5.4.2. Individual desorber and reboiler performance

Fig. 8 shows a comparison of the experimental desorber outlet liquid loading compared with the simulated loading. As previously noted only the liquid side measurements are available here. The figure shows that the agreement between experimental and simulated loadings is reasonable. However, this figure is somewhat misleading as small deviations from the diagonal may hide large discrepancies in percentage stripped in the desorber.

The majority of simulations show an under-prediction of the CO_2 transfer in the desorber column indicated by the higher values of the lean loading out of the column. For loading range 1 and the lower part of loading range 2, the agreement is good and no systematic deviation is visible. However, in loading ranges 2 and 3 the simulations systematically under-predict the performance of the desorber. As previously mentioned, this may be caused by experimental uncertainty associated with the liquid sampling out of the stripper. If flashing occurs, which is more likely in loading range 3, the sampled loading values

Table 3
Deviations simulations versus experimental runs

Run[a]	CO_2 mass transfer Exp	CO_2 mass transfer (base case) Sim	% dev Abs CO_2 (base case) x_i[b]	CO_2 mass transfer (inlet enthalpy assumption 2) Sim	% dev Abs CO_2 (inlet enthalpy assumption 2) x_i[b]
1	5.08	5.64	9.82	5.64	9.82
2	4.93	5.48	10.05	5.48	10.05
3	4.88	5.41	9.70	5.41	9.70
4	4.73	5.30	10.63	5.30	10.63
5	4.34	4.91	11.60	4.91	11.60
6	6.35	6.63	4.22	6.64	4.29
7	4.19	4.75	7.17	4.75	7.17
8	6.25	6.55	4.54	6.55	4.54
9	4.59	5.08	9.61	5.08	9.61
10	4.74	5.34	11.30	5.34	11.23
11	3.64	3.60	−1.03	3.60	−1.03
12	8.20	7.57	−8.33	7.90	−3.74
13	3.01	2.47	−21.74	2.65	−13.65
14	11.29	9.29	−21.60	11.56	2.32
15	3.91	3.59	−8.95	3.63	−7.63
16	5.74	5.12	−12.15	5.44	−5.62
17	11.46	10.05	−13.94	12.01	4.63
18	8.89	8.39	−6.05	10.03	11.30
19	7.34	7.81	6.01	7.81	6.01
AAD			9.91		5.79
AD			9.92		7.61

Absolute average deviation (AAD) and average deviation (AD) for the set of runs based on the average of the liquid and gas side mass transfer data.

[a]Sorted by date.

[b]$x_i = \frac{v_{sim} - v_{ex}}{v_{ex}} \cdot 100$.

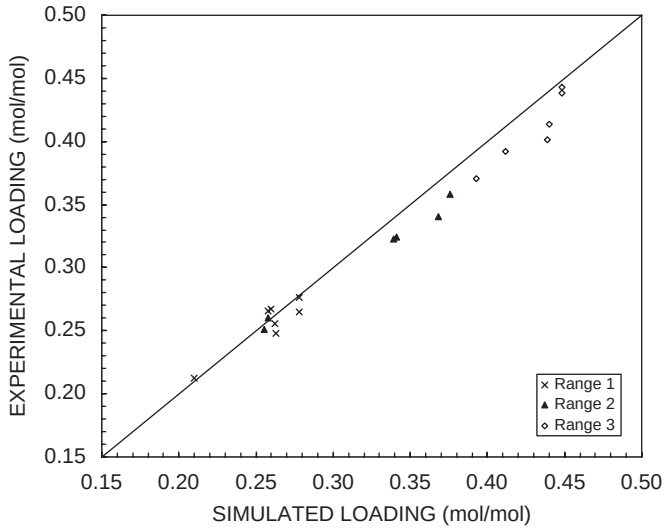

Fig. 8. Experimental and simulated lean loading out of the desorber column prior to the reboiler.

will be lower than the actual values, fictitiously showing up as under-predictions in the simulated results.

However, some of the discrepancies observed between simulations and experimental values may also be caused by our assumption of 100% efficiency in the reboiler. As was pointed out in the study of Tobiesen and Svendsen (2006), the desorber and reboiler seem, to some degree, to compensate for each other. If the performance of the desorber is reduced, the reboiler receives liquid at higher loading and removes more CO_2. A larger outlet reboiler CO_2 partial pressure will also cause a smaller driving force for stripping in the desorber. An "efficient" reboiler will therefore in itself cause less stripping in the desorber. It may well be that the reboiler efficiency varies with boil-up rate, circulation rate, and liquid loading into the reboiler. At low loadings, as already mentioned, more energy must be transferred per mol CO_2 released. However, under these conditions the change in loading in the reboiler will normally be small; therefore, the total effect will be a smaller need for heat. At high loading the change in loading will be high, requiring more heat to be transferred to the liquid, and possibly a lower efficiency. Likewise, a high liquid throughput will require more energy, indicating lower efficiency. In addition, also a low heat duty will work in the same manner. However, with the uncertainties in our data, more certain statements about these effects cannot be made.

Table 4 shows a comparison between the experimental and simulated reboiler temperatures. The simulated values are, apart from three readings, systematically higher than the experimental values by 0.7–4.8 °C. The average deviation is 2.7 °C, which is close to the deviation observed for the pure water tests. This leads to the conclusion that the model predicts the reboiler temperatures with acceptable accuracy. Table 4 also gives the measured and simulated desorber outlet temperatures. The measurement 10 cm from the packing bottom is used as a reference point. The desorber internal temperature readings were better calibrated than the reboiler reading and the accuracy

Table 4
Experimental and simulated temperatures for desorber bottom and reboiler

Run	T1 exp[a] (°C)	T1 sim (°C)	Reboiler	
			Temp exp (°C)	Temp sim (°C)
1	120.4	121.2	121	122.9
2	120.1	121.1	121	122.8
3	120.4	121.2	122	122.8
4	119.8	120.8	120	122.4
5	122.1	123.7	121.4	125.1
6	116.5	118.7	118.5	122.2
7	116.7	120.1	118	122.5
8	118.9	122.2	120.5	124.8
9	117.9	121.5	119.5	124.3
10	117.8	121.3	119.3	124
11	112.4	114.3	116.2	119.9
12	114.3	115.7	117.1	120.2
13	106.6	105.9	111.7	113.5
14	110.6	107.6	115.9	114.4
15	101.1	102.9	107.2	110.2
16	101.3	103	107.3	109.8
17	112.3	110.9	116	116.7
18	111.8	112.3	115.3	117.3
19	116.4	117.8	118.2	121.1

[a]T1 measured 10 cm above the bottom of desorber packing.

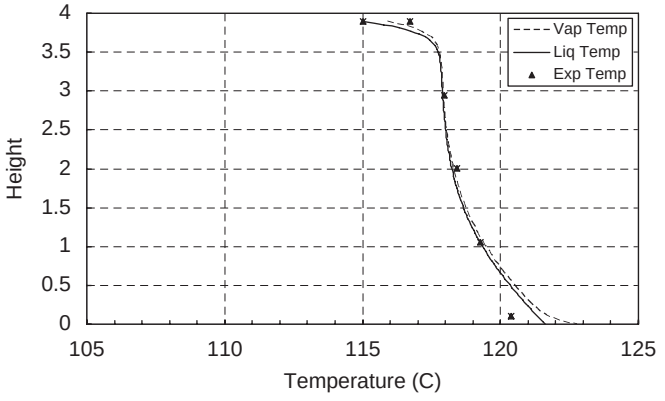

Fig. 9. Experimental and simulated desorber temperatures. Run 2, loading range 1.

is anticipated to be ±0.2 °C. One problem is the two-phase flow at this point making it uncertain whether the reading is for gas phase or liquid phase. However, the gas–liquid temperature difference is small; therefore, this uncertainty is disregarded and for the simulations, an average is used. As can be seen, the differences between measured and simulated values range from −3.0 to +3.6, with an average deviation of 1.2 °C. The under-predictions were for three cases in loading range 3 and are related to the choice of inlet enthalpy content as is discussed below. Overall, the values are deemed satisfactory.

5.4.3. Temperature profiles

The measured profiles shown in Figs. 9–11 for runs 2, 14, and 18, respectively, are taken to be an average for the liquid and vapor temperatures since it is not known which phase is in

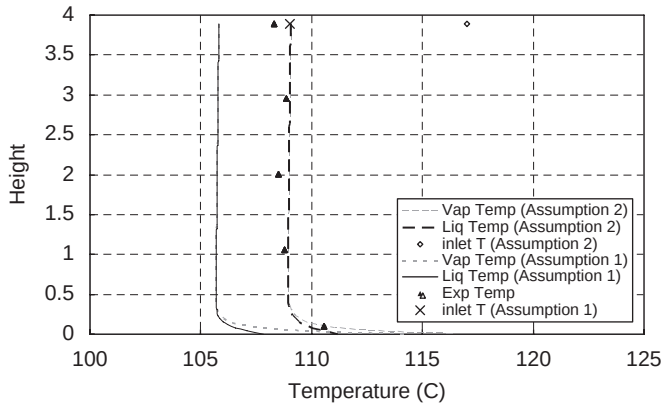

Fig. 10. Experimental and simulated desorber temperatures. Run 14, loading range 3.

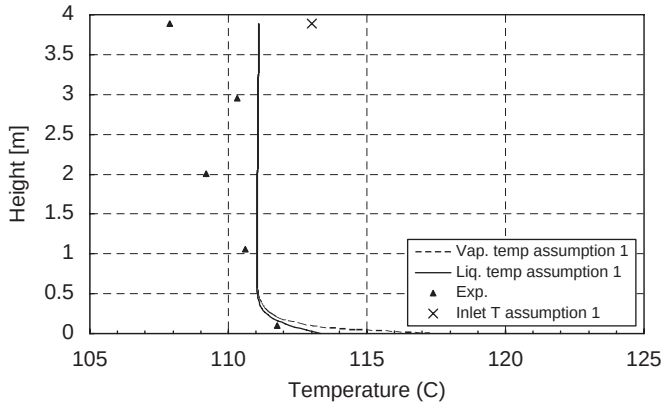

Fig. 11. Experimental and simulated desorber temperatures. Run 18, loading range 3.

contact with the sensor at any time. It should be noted that the temperature probe at 2 m consistently showed low temperatures and should be disregarded. Fig. 9 shows the desorber packing temperature profile for run 2. This is a run in loading range 1, and an equilibrium test, or isenthalpic flash, on the desorber inlet rich amine stream shows zero vapor fraction. This implies that our assumption of single-phase liquid is reasonable in this case. Fig. 9 shows that the simulated and experimental temperature profiles are in very good agreement. Similar agreement was found for all the runs in loading range 1 where a flash calculation predicted single-phase liquid at the desorber inlet rich amine temperature measurement point.

As noted earlier, when the inlet rich amine loading is high, the liquid may flash before entering the desorber, and thus the single-phase liquid assumption does not hold. Such a case is shown in Fig. 10, representing run 14, where assumption 1 indicates single-phase liquid inlet rich amine. It can be seen that with this assumption, the simulated temperature profile is much lower than the experimental one. This indicates that the enthalpy content of the inlet stream must have been higher than what was assumed, i.e. some flashing must have taken place before the temperature was registered. This is also reflected in the CO_2 mass transfer being under-predicted with 21.6% for this case. Assumption 2 in Fig. 10 is the other extreme, being that the inlet stream is in two-phase equilibrium at the temperature registration point. The dashed line indicates the results of the simulation with this assumption, and as can be seen, the agreement with the measured temperatures becomes very good. In addition, with this assumption, the resulting mass transfer deviation decreases to −2.7%. In run 14 the rich amine pre-heater was used (and of course also included in the simulations), and this might have aided the flashing.

In run 18, shown in Fig. 11, also in loading range 3, but in this case not using the pre-heater, the situation is opposite. The desorber inlet rich amine stream seems to be single-phase liquid as this is the assumption used in the simulation. The predicted temperature profile, even with the lowest possible inlet flow enthalpy content, is still higher than the experimental ones. Here, significant flashing seems to occur between the inlet rich amine desorber entrance and the packing, indicated by the large reduction in temperature from the inlet to the first measurement in the packing. It also seems that it takes some distance into the packing before the liquid is heated up to the desorber temperature. The model under-predicts the CO_2 stripping by 6%, which indicates that the inlet rich amine enthalpy content was somewhat underestimated and is opposite to what the temperature profile indicates.

These three cases, the first indicating single-phase liquid in the desorber inlet rich amine, the second where a large difference between these two simulations, based on the two different assumptions, was found, and the third where temperature profile and CO_2 stripped point in two different directions, show how important it is to have a well-defined inlet rich amine stream, not only with composition and temperature, but also with approach to equilibrium.

It should also be noted that in the loading range 3 cases shown, the temperature profiles in both runs indicate an underutilization and a pinch in the desorber in the upper section of the packing. In these runs there is hardly any stripping taking place in the desorber at all. Most of the stripping occurs in the reboiler. This is indicated by the almost constant temperature in the desorber. This was actually the case for most of the range 3 runs and was a consequence of the way the experiments were designed. The runs were designed to cover an operating line in the absorber, and the desorber would then have to cope with what it received. For example, at high rich amine loading, a high lean loading was also desired in order to operate at the high end of the operating line in the absorber. The opposite would be true for the low end. In hindsight it is clear that this is not the best way of obtaining data for desorber validation. On the other hand, data have been gathered for quite extreme desorber operating conditions, which expands the ordinary state space available for validation.

5.4.4. Simulations with inlet enthalpy assumption 2

In order to evaluate the effects of the inlet enthalpy assumption given for the base case, the data set was also simulated

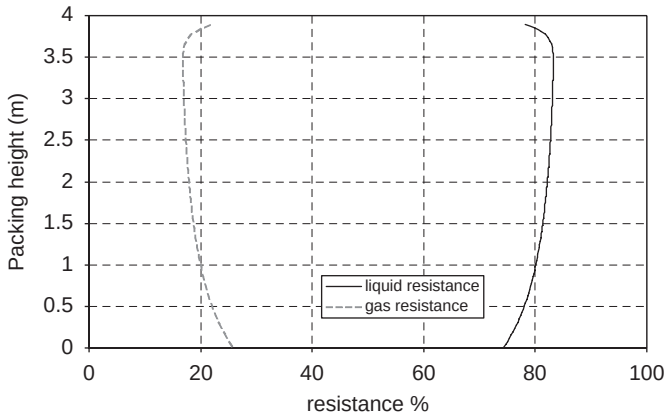

Fig. 12. Liquid and gas side resistances for the desorber packing. Run 2, loading range 1.

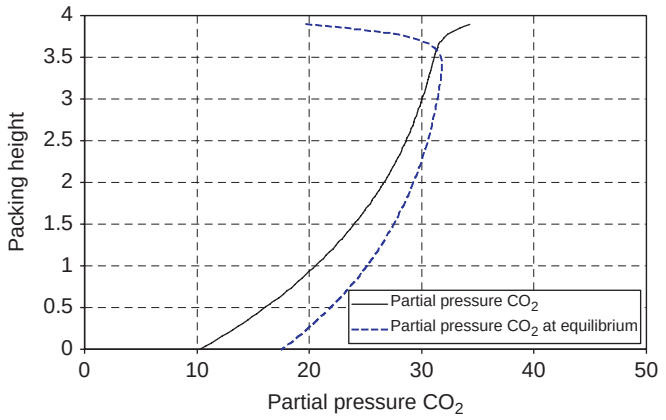

Fig. 13. Partial pressure profiles for the desorber packing. Run 7, loading range 2.

with enthalpy assumption 2 (assuming g/l equilibrium at the measured inlet temperature). It was found that the inlet enthalpy had to be increased for 7 of the 19 runs, runs 12–18, all of which were in loading range 3 except for run 12 which was in range 2. The mass transfer rates given in Table 3 show that using assumption 2 has no effect on the 11 first runs as well as on run 19, but that the additional inlet enthalpy causes a higher degree of mass transfer at the higher loading runs. This results for the total data set in an AAD and AD of 5.79% and 7.61%, respectively. From this it is clear that many of the high loading runs were already in the two-phase flow at the inlet to the desorber and that assumption 2 provides a better fit to the data as a whole. However, in the following, assumption 1 is still used as the base case.

5.4.5. Liquid film resistance and driving forces in desorber

Desorption in chemical absorbents is normally strongly influenced by the liquid film resistance. The fraction of the liquid film resistance is defined as in Tobiesen et al. (2007):

$$\mathrm{res}_{L,\mathrm{CO_2}} = \frac{\dfrac{1}{Ek_{\mathrm{CO_2}L}}}{\dfrac{1}{Ek_{\mathrm{CO_2}L}} + \dfrac{1}{k_{\mathrm{CO_2}G} H_{\mathrm{CO_2}}}}, \tag{8}$$

where $Ek_{\mathrm{CO_2}L}$ is the product of the liquid mass transfer coefficient for physical absorption and the enhancement factor due to chemical reaction.

Fig. 12 shows the liquid- and gas-phase resistances for run 2 in loading range 1. The liquid-phase resistance is highest (80–90%) in the middle part of the column while the largest resistance in the gas phase is at the top and bottom of the column. This is typical for most of the runs, but the liquid-phase resistance is reduced to below 70% in some cases. Because of the very fast chemical reactions, the gas side contribution to the overall resistance is larger than what was observed in the absorber for the same runs. In Fig. 13 it can be seen that there is a rich end pinch in run 7, also indicated by a slight decrease in liquid-phase resistance for run 2 as shown in Fig. 12. A rich end pinch occurs for the experimental runs in the high loading

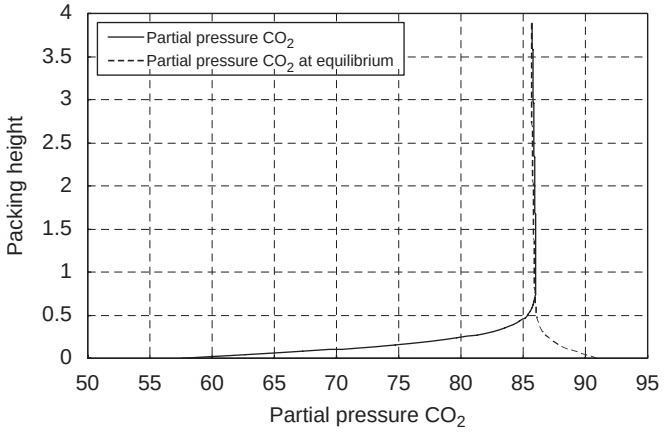

Fig. 14. Partial pressure- and equilibrium curves for the desorber packing. Run 19, loading range 3.

range. At medium and low loadings, as exemplified by run 7, Fig. 13, however, significant desorption occurs in the column as shown by the changes in partial pressure along the packing. Absorption is seen to occur in the very top section, and at this point in the column the section provides only sensible heat to the solvent from the steam until it reaches a point where there is a driving force for desorption. This is a trend through many of the runs in loading ranges 1 and 2 while in loading range 3 there is very little stripping at the top of the column at all, as typically seen from run 19 in Fig. 14, where a pinch is reached at about 0.5 m from the bottom of the column. The upper section of the stripper has hardly any effect on stripping in these cases as there is no driving force for desorption. For the cases in range 3, the experimental data provide a good basis for validation of the equilibrium model at high loadings. Similar rich end pinches are reported from pilot experiments by Dugas et al. (2006) and from simulations by Freguia and Rochelle (2003). For the cases at medium and lower loadings, such as the one shown in Fig. 13, the experimental data also provide a good representation of the actual desorption rate along the packing. The

Table 5
Percent of experimental-simulated mass transfer deviation for desorber and reboiler

Run	Model: Hoff et al. (2004) Data: Jou et al. (1995) x_i [a]	Model: Deshmukh–Mather (1981) Data: Weiland et al. (1993) x_i [a]	Model: Deshmukh–Mather (1981) Data: Tobiesen et al. (2007), Ma'mun (2005) x_i [a]	Base case model $w/\gamma_{H_2O}=1$ x_i [a]	Base case model w/γ_{H_2O} reduced 3% x_i [a]
1	−5.40	12.75	9.18	6.69	11.62
2	−5.54	14.05	10.84	6.99	11.82
3	−6.09	13.71	10.51	6.67	11.50
4	−5.70	14.46	11.36	7.48	12.59
5	−7.60	11.04	10.56	7.36	14.44
6	−8.03	10.18	6.76	3.39	4.48
7	−12.29	13.36	11.05	4.61	8.70
8	−11.41	9.69	7.34	2.03	6.05
9	−3.58	12.12	8.50	6.86	11.07
10	−1.02	13.99	10.41	8.74	12.59
11	−13.21	4.13	−1.52	−0.78	−1.27
12	−21.30	−3.51	−9.47	−8.39	−8.64
13	−47.45	−8.43	−21.96	−19.61	−23.06
14	−44.13	−11.22	−22.82	−20.23	−22.59
15	−45.33	8.65	−8.29	−6.34	−10.72
16	−52.68	7.15	−10.91	−9.24	−13.91
17	−31.89	−6.88	−15.71	−13.00	−14.69
18	−24.47	0.47	−8.79	−5.06	−6.84
19	−8.46	8.54	3.40	5.43	6.12
AAD	14.34	6.81	10.49	7.98	11.12
AD	18.72	9.70	10.49	7.84	11.19

[a] $x_i = \frac{v_{sim} - v_{ex}}{v_{ex}} \cdot 100.$

experimental runs thus include data for validation of both the equilibrium model up to about 123C and high loadings as well as for validation of the mass transfer model and the calorific features of the model. The correlations used for estimation of hydraulics, in particular the gas/liquid contact area, are developed mainly for distillation and not for reactive absorption. In absorption and desorption the gas/liquid flow ratio is much higher than that for distillation processes. These hydraulic correlations are therefore main uncertainties in the model. A key research task is therefore to obtain correlations based on reactive absorption/desorption systems for the respective solvents used.

5.4.6. Equilibrium data

As shown by Tobiesen et al. (2007), the single most important factor when simulating an absorber is the equilibrium model. This is even more important for desorption since all reaction and transport rates are much higher. Therefore, four different equilibrium models or model fits were tested. In addition to the base case model described earlier, the Deshmukh–Mather model was tested using the parameters given by Weiland et al. (1993) as well as refitted to data from Tobiesen et al. (2007) and Ma'mun et al. (2005). As the fourth case, the Hoff et al. (2004) model was fitted to data by Jou et al. (1995). When the Deshmukh–Mather model was refitted to data from Tobiesen et al. (2007) and Ma'mun et al. (2005) the results matched the Hoff et al. (2004) model fitted to the same data.

Table 5 summarizes the simulation results for the combined desorber and reboiler and gives the AAD and AD for the data set for the three other equilibrium models from the base case. Although hardly any difference in CO_2 partial pressure was visible between the Hoff et al. (2004) model and the Deshmukh–Mather model fitted to the same data, they show a small difference when simulating the desorber. The Hoff et al. (2004) model shows both an AAD and an AD of 9.9% (see Table 3), and the Deshmukh–Mather modes gives 10.5% for both values. Both seem equally good indicating that it may not be of much use to use a rigorous equilibrium model compared with a simplified equilibrium model for desorber evaluations. This is not surprising as kinetics were assumed instantaneous such that only the CO_2 activity driving force, interface CO_2 concentration, component diffusivity ratios, and the bulk free MEA concentration enter into the mass transfer rate expression.

The Deshmukh–Mather model with the interaction parameters of Weiland et al. (1993) shows the smallest deviations from the experimental data with AAD and AD of 6.8% and 9.7%, respectively. This model seems to over-predict the CO_2 partial pressures at high loading being above the experimental points of both Jou et al. (1995) and Ma'mun et al. (2004). As indicated by the large difference between the AAD and AD values, systematic deviations exist. This is clear from Table 5 as stripping in range 1 and the lower part of range 2 is over-predicted, whereas at higher loadings, upper range 2 and range 3, the stripping is well predicted or under-predicted. This is in line with the over-prediction of CO_2 partial pressure that this model seems to give at low and intermediate loadings.

The Hoff et al. (2004) model fitted to data from Jou et al. (1995) shows by far the largest deviations with AAD and AD of 14.3% and 18.7%, respectively. The deviations from experimental results are particularly large in loading range 3 resulting in the systematic deviation indicated by the difference in AAD and AD. The high rich loading deviations are consistent with data of Jou et al. showing the lowest partial pressures in the whole loading range, but in particular at high loadings.

It can be concluded that also for desorption, the equilibrium data model is vital for obtaining good simulation results. As previously mentioned, the rigorousness of the model may not be so important as long as it represents the VLE data well and of course as long as the data are good. This means that simplified models may be used, significantly reducing the computational load. However, a more rigorous model should include the effect of the activity coefficient of water, as will be discussed shortly.

5.4.7. The effect of activity coefficient for water

In the base case equilibrium description of MEA and water, the respective activity coefficients were obtained from a fit to experimental binary data from Nath and Bender (1983) up to about 90 °C using a Wilson correlation and extrapolated to 120 °C. This model does not account for the impact of ionization of species when CO_2 is absorbed into the solution and the subsequent changes in amine and water molar fraction and activity. These discrepancies could be significant at temperatures in excess of 100 °C. The resulting activity coefficient for water using this correlation varies from 0.94 to 0.96 depending on the solution temperature and amine concentration. The activity coefficient for MEA varies from 0.30 to 0.70 but a change in the values for MEA will not result in overall changes in the desorber and reboiler performance. However, only small changes in the activity coefficient for water will result in significant changes in overall stripping. Table 5 summarize results for the whole data set when the activity coefficient is either assumed unity or reduced by 3% from the obtained value from the Wilson correlation. Assuming that the water activity increases with CO_2 loading, which is not unreasonable, in this case to a value of 1, gives AAD and AD of 7.98% and 7.84%, respectively. The improvement is most significant in loading range 1, but is seen in all runs. A reduction in the activity coefficient with 3% yields an AAD and AD of 11.12% and 11.19%, respectively, implying a reduction in the model quality. The effect of the water activity coefficient is thus significant, which is not surprising as the water content is as high as nearly 89 mol% in 30 wt% MEA. Thus, although a simplified equilibrium model can be used, it is important to include the activity coefficient for water.

6. Conclusions

A model for CO_2 desorption including desorber packing, reboiler, and condenser was developed and validated against pilot plant data for the system of 30 wt% monoethanolamine (MEA) solution. Two VLE models were used, the Deshmukh–Mather model, and the model of Hoff et al., fitted towards two sources of equilibrium data. The interface mass transfer model used assumes reversible instantaneous chemical reaction, and thermal, transport and hydraulic properties were used as given in Tobiesen et al. (2007). The model was validated against a database from a laboratory scale pilot plant, constituting 19 runs. Mass transfer data for both liquid and gas were obtained as well as temperature profiles in the desorber column. Runs with pure water enabled check of the heat balance and estimation of the heat losses in the unit. Average absolute deviation (AAD) and absolute deviation (AD) between gas and liquid side for the data set were found to be 4.21 and 4.48, respectively. This was deemed acceptable and taken as a support for the quality of the experimental data. Slightly higher deviations were found in the high loading range than for low and medium loadings (< 0.4). Reboiler heat duties ranged from 11 to 3.7 MJ/kg CO_2 removed, the highest values for low loadings (0.26–0.29). Analysis of the desorber section liquid outlet allowed individual evaluation of desorber and reboiler. It was found difficult to use these data as they are extremely hard, if at all possible, to obtain sufficient accuracy in the desorber outlet loading reading, to justify a detailed comparison with simulated values. However, it was found that the degree of stripping in the desorber column compared with reboiler decreases with increasing rich loading and that the percentage CO_2 removed in the desorber decreases with decreasing heat duty.

The agreement between the experimental averaged and the simulated CO_2 mass transfer rate was found to be good, with an AAD and AD of 9.92% and 9.91%, respectively. The simulations slightly over-predict mass transfer in the low loading ranges and under-predict mass transfer in the high loading range. A comparison of simulated and measured reboiler temperature showed good agreement. In addition, simulated and measured desorber temperature profiles agree very well for the low loading ranges where the desorber inlet liquid flow was well characterized. In cases where flashing of the desorber inlet flow can occur, it was found extremely important not only to know flow composition, rate, and temperature, but also the enthalpy content.

Liquid side mass transfer restrictions were found to dominate, but the gas side mass transfer resistance was significantly more important in desorption than for absorption of CO_2 into MEA. Desorber rich end pinches were found for most of the runs at low and medium loading and mass transfer reversal, meaning absorption, was detected towards the top of the packing in several cases. In the high loading range pinches were found to occur lower down in the desorber, and in several cases very little stripping occurred in the desorber but was rather stripped off in the reboiler.

Using four different equilibrium models (two different VLE models fitted to two different data sets), it was shown that a simplified and a rigorous model, when fitted to the same data, would give very similar desorption performance predictions. The data used for fitting were found to be very important and AAD and AD varying from about 8% to 18% were obtained

Table A1
Experimental stream data from pilot plant

Run	Loading range	Rich stream inlet		Liquid stream out desorber		Liquid stream out reboiler		MEA[a] conc. (kmol/m^3)
		Temp.[b] (°C) (mol/mol)	Loading	Temp.[b] (°C) (mol/mol)	Loading	Temp. (°C) (mol/mol)	Loading	
1	1	115	0.316	121	0.267	121.0	0.219	5.1
2	1	115	0.315	121	0.248	121.0	0.221	5.0
3	1	115	0.313	119	0.256	122.0	0.218	4.9
4	1	115	0.309	118	0.266	120.0	0.218	4.9
5	1	116	0.264	121	0.213	121.4	0.182	4.9
6	2	115	0.365	117	0.325	118.5	0.277	4.6
7	1	115	0.295	118	0.276	118.0	0.238	4.7
8	1	118	0.312	120	0.265	120.5	0.227	4.7
9	2	115	0.329	119	0.251	119.5	0.214	5.0
10	2	115	0.338	119	0.260	119.3	0.216	4.9
11	2	112	0.396	114	0.358	116.2	0.304	5.0
12	2	113	0.392	115	0.340	117.1	0.291	5.0
13	3	106	0.445	106	0.413	111.7	0.375	5.1
14	3	109	0.457	109	0.401	115.9	0.366	5.1
15	3	103	0.450	101	0.438	107.2	0.402	5.1
16	3	104	0.451	102	0.443	107.3	0.406	5.1
17	3	111	0.429	111	0.392	116.0	0.337	5.1
18	3	113	0.407	111	0.370	115.3	0.337	5.2
19	2	116	0.350	116	0.323	118.2	0.291	5.2

[a]MEA concentration is assumed to be constant for the liquid streams. Pressure drop over reboiler is assumed to be negligible. Stream pressures found in Table A2. [b]Temperatures measured to whole degrees.

Table A2
Experimental data from pilot plant

Run	Reboiler			Condenser		Condensate rate (kg/h)	CO_2 flow rate top (kg/h)	Liquid load (m^3/m^2/h)
	Duty (kW)	T (°C)	P (kPa (abs))	T[a] (°C)	P (kPa (abs))			
1	11.6	121.0	198.0	15	196.5	8.0	5.1	7.64
2	11.6	121.0	197.0	13	195.5	8.1	5.0	7.64
3	11.5	122.0	198.0	15	196.5	8.0	4.9	7.64
4	11.6	120.0	195.0	15	193.5	8.6	4.8	7.64
5	13.5	121.4	206.5	15	205.0	11.1	4.4	7.64
6	11.6	118.5	213.5	16	212.0	6.5	6.2	11.46
7	11.8	118.0	202.0	18	200.5	8.1	4.6	11.46
8	13.8	120.5	217.0	19	215.5	9.8	6.2	11.46
9	9.6	119.5	204.6	12	203.6	5.9	4.7	5.73
10	9.7	119.3	203.6	12	202.6	6.1	4.7	5.73
11	5.8	116.2	207.0	11	206.0	2.5	3.6	5.73
12	11.6	117.1	205.0	18	203.0	5.9	8.3	11.46
13	3.9	111.7	209.4	12	208.4	0.0	3.2	5.73
14	11.6	115.9	215.4	22	212.4	4.3	11.5	17.20
15	5.8	107.2	202.1	12	200.1	0.0	3.9	11.46
16	7.9	107.3	201.2	15	199.2	0.0	6.1	17.20
17	13.4	116.0	205.8	31	203.8	5.9	11.7	17.20
18	11.7	115.3	204.7	19	202.7	5.4	9.1	17.20
19	13.6	118.2	206.7	22	204.7	8.0	7.4	17.20

[a]Temperatures measured to whole degrees. The reboiler and column have been corrected for heat loss and reflux cooling, which is maintained by the energy balances of the units.

depending on the fit. The activity coefficient of water was found to have a strong influence on the agreement with experimental data. An increase in the activity coefficient of about 5% reduced the AAD and AD from the base case values of about 10% to 8.0% and 7.8%, respectively.

Notation

A,B,C,D	main chemical components
C_A	concentration component A, kmol/m^3
D_i	Fick diffusion coefficient, m^2/s

E	enhancement coefficient, dimensionless
H_i	Henry coefficient of component i
k_{CO_2L}	liquid mass transfer coefficient for physical absorption
K	equilibrium constant
N	interfacial molar flux, kmol/(m^{2}s)
p_i	partial pressure of component i, kPa
r_j	ratio of absorbent to solute diffusivity
T	temperature, K or °C

Subscripts

j	components undergoing mass transfer, or chemical reaction number
l, g	liquid, gas phase

Superscripts

b	bulk liquid
eq. and *	at equilibrium
in	gas/liquid interface

Acknowledgements

The financial support for this work by the Research Council of Norway Klimatek Project through the SINTEF Project 661292 and by the European Commission through the CASTOR Integrated Project (Contract no. SES6-CT-2004-502856) is greatly appreciated. The authors also acknowledge the help of Karl Anders Hoff with the equilibrium model.

Appendix A.

Tables A1 and A2 presents the experimental data for all runs.

References

Astarita, G., Savage, D.W., 1980a. Theory of chemical desorption. Chemical Engineering Science 35, 649–656.

Astarita, G., Savage, D.W., 1980b. Gas absorption and desorption with reversible instantaneous chemical reaction. Chemical Engineering Science 35, 1755–1765.

Billett, R., Schultes, M., 1999. Prediction of mass transfer columns with dumped and arranged packings. Transactions of the Institution of Chemical Engineers, Part A 77, 498–504.

Bird, R.B., Steward, W.E., Lightfoot, E.N., 1960. Transport Phenomena. first ed.. Wiley, New York.

Bosch, H., Versteeg, G.F., van Swaaij, W.P.M., 1990. Desorption of acid gases CO_2 and H_2S from loaded alkanolamine solutions. In: Vansant, E.F., Dewolfs, R. (Eds.), Process Technology Proceedings, vol. 8, on Gas Separation Technology. Elsevier Science Publishers, Amsterdam.

Burkhardt, T., Camy- Portenabe, J., Fradet, A., Tobiesen, F.A., Svendsen, H.F., 2006. Optimization of the process loop for CO_2 capture by solvents. In: Proceedings of the GHGT-8: 8th International Conference on Greenhouse Gas Control Technologies, Trondheim, Norway, 19–22 June.

Cadours, R., Bouallou, C., Gaunand, A., 1997. Kinetics of CO_2 desorption from highly concentrated and CO_2-loaded methyldiethanolamine aqueous solutions in the range 313–383 K. Industrial and Engineering Chemistry Research 36, 5384–5391.

Chakma, A., 1999. Formulated solvents: new opportunities for energy efficient separation of acid gases. Energy Sources 21, 51–62.

Danckwerts, P.V., 1971. Gas Liquid Reactions. McGraw-Hill, New York, USA.

De Brito, M.H., von Stockar, U., Bangerter, A.M., Bomio, P., Laso, M., 1994. Effective mass-transfer area in a pilot plant column equipped with structured packings and with ceramic rings. Industrial and Engineering Chemistry Research 33, 647–656.

Deshmukh, R.D., Mather, A.E., 1981. A mathematical model for equilibrium solubility of hydrogen sulfide and carbon dioxide in aqueous alkanolamine solutions. Chemical Engineering Science 36, 355–362.

Dugas, R.E., Rochelle, G.T., Seibert, F., 2006. CO_2 capture performance of a monoethanoloamine pilot plant. In: Proceedings of the GHGT-8: 8th International Conference on Greenhouse Gas Control Technologies, Trondheim, Norway, 19–22 June.

Freguia, S., Rochelle, G.T., 2003. Modeling of CO_2 capture by aqueous monoethanolamine. A.I.Ch.E. Journal 4, 1676–1686.

Glasscock, D.A., Rochelle, G.T., 1991. CO_2 absorption/desorption in mixtures of methyldiethanolamine with monoethanolamine or diethanolamine. Chemical Engineering Science 46, 2829–2845.

Hoff, K.A., Juliussen, O., Falk-Pedersen, O., Svendsen, H.F., 2004. Modeling and experimental study of carbon dioxide absorption in aqueous alkanolamine solutions using a membrane contactor. Industrial and Engineering Chemistry Research 43, 4908–4921.

Jou, F.Y., Mather, A.E., Otto, F.D., 1995. The solubility of CO_2 in a 30 mass percent monoethanolamine solution. Canadian Journal of Chemical Engineering 73, 140–147.

Kershenbaum, L.S., Escobillana, G.P., Saes, J.A., Perez-Correa, J.R., Neuburg, H.J., 1991. Behaviour of absorption/stripping columns for the CO_2–MEA system, modelling and experiments. Canadian Journal of Chemical Engineering 69, 969–977.

Ma'mun, S., Nilsen, R., Svendsen, H.F., Juliussen, O., 2005. Solubility of carbon dioxide in 30 mass% monoethanolamine and 50 mass% methyldiethanolamine solutions. Journal of Chemical Engineering Data 50, 630–634.

Nath, A., Bender, E., 1983. Isothermal vapor–liquid equilibria of binary and ternary mixtures containing alcohol, alkanolamine and water with a new static device. Journal of Chemical Engineering Data 28, 370–375.

Olander, D.R., 1960. Simultaneous mass transfer and equilibrium chemical reaction. A.I.Ch.E. Journal 6, 233–239.

Rocha, J.A., Bravo, J.L., Fair, J.R., 1993. Distillation columns containing structured packings: a comprehensive model for their performance. 1. Hydraulic models. Industrial and Engineering Chemistry Research 32, 641–651.

Rocha, J.A., Bravo, J.L., Fair, J.R., 1996. Distillation columns containing structured packings: a comprehensive model for their performance. 2. Mass-transfer model. Industrial and Engineering Chemistry Research 35, 1660–1667.

Sakwattanapong, R., Aroonwilas, A., Veawab, A., 2005. Behavior of reboiler heat duty for CO_2 capture plants using regenerable single and blended alkanolamines. Industrial and Engineering Chemistry Research 44, 4465–4473.

Tobiesen, A.F., Svendsen, H.F., 2006. Study of a modified amine based regeneration unit. Industrial and Engineering Chemistry Research 45, 2489–2496.

Tobiesen, F.A., Svendsen, H.F., Juliussen, O., 2007. Validation of a rigorous model for carbon dioxide absorption in structured packings. A.I.Ch.E. Journal 53, 846–865.

Weiland, R.H., Rawal, M., Rice, R.G., 1982. Stripping of carbon dioxide from monoethanolamine solutions in a packed column. A.I.Ch.E. Journal 28, 963–972.

Weiland, R.H., Chakravarty, T., Mather, A.E., 1993. Solubility of carbon dioxide and hydrogen sulfide in aqueous alkanolamines. Industrial and Engineering Chemistry Research 32, 1419–1430.